Synthesis, characterization and molecular docking studies of nickel(II) complexes derived from 4-amino-5-mercapto-3-methyl-1,2,4-triazole: In vitro antimicrobial and anticancer activities

Sachin A. Deodware
Shri Shivaji Mahavidyalaya
panchsheela Ashok ubale (panchsheela_ubale@rediffmail.com)
Orchid College of Engineering and Technology Solapur: Nagesh Karajagi Orchid College of Engineering and Technology https://orcid.org/0000-0002-9513-0398
Umesh B. Barache
Shri Shivaji Mahavidyalaya
Pratibha C. Dhale
Shri Shivaji Mahavidyalaya
Kundalkesha D. Gaikwad
Shri Shivaji Mahavidyalaya
Umakant B. Chanshetti
Shri Shivaji Mahavidyalaya
Shashikant H. Gaikwad
Shri Shivaji Mahavidyalaya

Research Article

Keywords: nickel(II) complexes, spectral studies, molecular docking, anticancer screening, antimicrobial studies

Posted Date: May 4th, 2021

DOI: https://doi.org/10.21203/rs.3.rs-471368/v1

Abstract

A series of nickel(II) complexes (C_1-C_3) with Schiff bases (HL_1-HL_3) derived from 4-amino-5-mercapto-3-methyl-1,2,4-triazole and 2/3/4-nitrobenzaldehyde having composition $[Ni(L)_2(H_2O)_2]$ are reported and characterized based on elemental analysis, magnetic moment study, spectral (electronic, FT-IR, ^{1}H-NMR) and thermal analysis. The spectroscopic studies reveal that Schiff bases behave as a monoanionic bidentate ligands towards the nickel(II) ion. Elemental analysis, spectral analysis, magnetic moment study and thermal analysis suggest the octahedral geometry of all the nickel(II) complexes. The thermal behaviour of complexes has been studied by TG and agrees with the composition of complexes. The Schiff bases and nickel(II) complexes have been screened for their antibacterial (*Staphylococcus aureus* and *Pseudomonas aeruginosa*) and antifungal (*Aspergillus niger* and *Candida albicans*) activity by MIC method. All the synthesized compounds were evaluated for molecular docking study and suggest nickel(II) complexes are acting as potential anticancer agents. Further, these compounds have been screened for their anticancer activity using OVCAR-3 cell line. Molecular docking study exhibit that the complexes are more active than the ligands.

Highlights

1. Schiff base ligands (HL_1-HL_3) and its nickel(II) complexes (C_1-C_3) are synthesized.
2. Synthesized compounds were characterized by elemental analysis, spectral analysis, magnetic moment study and thermal analysis.
3. Biological activities implies that Ni(II) complexes are more potent than their parent ligands.
4. In general all ligands and their complexes exhibit antibacterial and antifungal activity.
5. The anticancer activity supported by molecular docking study suggests that Ni(II) complexes exhibit potential anticancer agents.

1. Introduction

In 1965, Rosenburg discovered a platinum complex, cisplatin, which establish a revolution in the treatment of cancer. After this discovery, there is a considerable increase in the use of metal complexes in the treatment of cancer. Recently, study associated with metal containing drugs, showed promising biological activities[1]. A literature survey revealed that metal complexes synthesized from chelating agent and transition metal salts exhibit enhanced physico-chemical and pharmacological properties[2–4]. Heteroatoms of chelating agent on reaction with positively charged metal ions produce complexes with well-defined geometries that can interact with biomolecules[5]. The coordination compounds of 1,2,4-triazoles have a considerable interest because of their brilliant coordination potential and diverse pharmacological properties[6–14]. The presence of an electron withdrawing group like -NO_2 on aromatic ring showed improved antimicrobial activity[15, 16]. Due to their rich and all around coordination mode, we applied some triazole derivatives for the determination of trace amounts of precious metals like Cu(II),

Pd(II), Au(III), toxic metals like Se(IV), Te(V), Bi(III) and Cr(VI) [17–23]. There are also some known drugs containing 1,2,4-triazole moiety like Letrozole, Anastrozole[24], Trazodone[25, 26].

Literature survey reveals that, no work has been reported on the synthesis of nickel(II) complexes derived from 4-amino-5-mercapto-3-methyl-1,2,4-triazole and 2/3/4-nitrobenzaldehyde. Recently, in 2017 we reported[27] the synthesis and characterization of a series of cobalt, nickel and copper complexes of bidentate Schiff base derived from the condensation reaction of 4-amino-5-mercapto-3-methyl-1,2,4-triazole with 2-nitrobenzaldehyde and their utilization as an anticancer agent. Interestingly, it was found that Schiff base and its Co(II), Ni(II) and Cu(II) complexes exhibit excellent activity against breast cancer cell line MCF-7. Such results prompted us to design new compounds and aiming to get new anticancer agents.

Novel Schiff bases (HL_1-HL_3) and their nickel(II) complexes (C_1-C_3) were synthesized and characterized with the aid of elemental analysis, crystallographic, magnetic moment measurements, spectroscopic and thermogravimetric approaches. The present manuscript deals with the synthesis of nickel(II) complexes and their anticancer screening on the OVCAR-3 cell line, while antibacterial and antifungal screening by MIC. Thus, our study will provide innovative valuable insights for designing drugs for anticancer treatment.

2 Experimental

2.1 Materials and Methods

All the chemicals used were of AR grade and obtained from Sigma-Aldrich and Merck. All the solvents distilled before use as per recommended procedure. The melting points are taken into open capillaries at the Ambassador melting factor apparatus. The purity of synthesized compounds was routinely checked by thin layer chromatography (TLC) with silica gel-G (Merck). The instruments used for obtaining the spectroscopic data were IR–Thermo Fisher Scientific model Nicolet iS10; ^{1}H-NMR (DMSO, 400 MHZ) NMR spectrometer Bruker Avalce. TMS was used as an internal standard. The electronic spectra of ligand and complexes in DMSO were recorded on Shimadzu UV-3600. The thermograms of complexes have been recorded in the temperature range 50-1000 ^oC using Shimadzu DTG-60 H thermal analyzer at a heating rate of 10 ^oC min^{-1} under an oxygen atmosphere. Mass spectra of the compounds were recorded on TOF-ES technique at 70 ev using ESI/APCI-hybrid mass spectrometer.

The reagents required to perform *in vitro* anticancer Sulforhodamine B (SRB) assay such as RPMI-1640, minimum essential medium (MEM), 10% fetal bovine serum, dimethyl sulfoxide (DMSO), Sulforhodamine etc. were procured from Sigma and Hi Media Ltd. India. Further, a stock solution of 100 µg/mL of the all the test compounds were prepared by dissolving in 0.1% DMSO. The compounds were serially diluted and treated to the cancer cells. For cells culture, we have grown the cells and maintained in appropriate medium at pH 7.4, supplemented with 10% fetal bovine serum, glutamate (2 mM), acetic acid (1%). The

cell cultures used in this study were grown in a carbon dioxide incubator (Heraeus, GmbH, Germany) at 37°C with 90% humidity and 5% CO_2.

2.2 Chemical Synthesis

2.2.1. Synthesis of ligands (HL_1-HL_3)

4-Amino-5-mercapto-3-methyl-1,2,4-triazole (AMET) was prepared by reported method[28]. The Schiff bases (HL_1-HL_3) of (2'/3'/4'-nitrobenzalideneimino)-3-methyl-5-mercapto-1,2,4-triazole has been prepared by dissolving 2/3/4-nitrobenzaldehyde (1.511 g, 0.01 mol L^{-1}) and 4-Amino-5-mercapto-3-methyl-1,2,4-triazole (1.44 g, 0.01 mol L^{-1}) in 25 mL ethyl alcohol separately. The two ethanolic solutions were mixed thoroughly. The mixture was refluxed on a water bath for 3 h. The progress of reaction was checked by using TLC. On cooling, a crystalline chelating ligands (HL_1-HL_3) turned into separated with the aid of filtration, washed with cold ethanol and recrystallized from ethanol and dried in vacuum over anhydrous $CaCl_2$ (Scheme-1). The melting point of Schiff base HL_1=224 ^oC, HL_2=230 ^oC and HL_3=235 ^oC.

2.2.2. Synthesis of Metal Complexes (C_1 - C_3):

The Schiff bases *(HL_1 - HL_3)* (2.770 g, 0.01 mol L^{-1}) were dissolved in 25 mL ethanol and added to nickel chloride solution (1.188 g, 0.005 mol L^{-1}) respectively. The mixture was refluxed for 4h. The products formed were filtered and purified thoroughly with absolute ethanol and ultimately with acetone and dried in vacuum over anhydrous $CaCl_2$ (Scheme-1).

Scheme 1: Proposed structure of nickel(II) metal complexes (C_1 – C_3)

2.3. Biological studies

2.3.1.In vitro antimicrobial studies

The antibacterial and antifungal activities of the Schiff bases (HL_1-HL_3) and their metal complexes (C_1 – C_3) were tested on *Staphylococcus aureus, Pseudomonas aeruginosa* and *Aspergillus niger, Candida albicans* respectively. The method used for antibacterial activity was the Agar Well-Diffusion method[29] and for the antifungal activity Agar-Ditch method [30]. The stock solution having concentration of 1mg mL^{-1} was prepared and was used to prepare concentrations of 0.8, 0.6, 0.4, 0.2 mg mL^{-1}. The bacteria and fungi were inoculated on the surface of Nutrient agar and Sabouraud's agar respectively. The various concentrations of the compounds were inoculated in the wells prepared on the agar plates. The plates were incubated at room temperature for 24 h. To clarify the effect of DMSO on the biological screening, separate studies were carried out with DMSO and showed no activity against any bacteria and fungi.

2.3.2 Molecular Docking Studies:

Molecular docking is one of the most frequently used methods in SBDD because of its ability to predict, with a substantial degree of accuracy, the conformation of small-molecule ligands within the appropriate target binding site[31]. Following the development of the first algorithms in the 1980s, molecular docking is became an essential tool in drug discovery [32]. For example, the investigations involving crucial molecular events, including ligand binding modes and the corresponding intermolecular interactions that stabilize the ligand-receptor complex, can be conveniently performed[33]. Furthermore, molecular docking algorithms executes quantitative prediction of binding energetics, providing rankings of docked compounds based on the binding affinity of ligand-receptor complexes[32,33].

To find out the possible mode of action of the synthesized Schiff bases (HL_1-HL_3) and nickel(II) complexes (C_1-C_3) molecular docking calculations were carried out using biopredicta module of the V life MDS 4.4 on the crystal structure of the Human CDK 7 (PDB ID: IUA2) downloaded from Protein Data Bank (www.rcsb.org/pdb) at a resolution of 3.02.The protein structure was refined via deletion of all the hetero atoms including water molecules and the addition of the polar hydrogen atoms to get a native conformation. All other bonds were allowed to be rotatable. The structures of the synthesized metal complexes are drawn in the builder module of the V life MDS 4.4 engine. The 2D structures of the molecules were converted into the 3D structures and optimized via application of the MMFF force field. These optimized structures were further utilized for the docking analysis. All the calculations were performed on an Intel i3, based machine running windows 7 as the operating system. The docked protein-ligand complex was further analysed via docking score of each of the complex, which is nothing but the binding energy of the complex, for every derivative 100 binding conformations were analysed to select the best conformation having the minimum docking score.

2.3.3.Antiproliferative activities against OVCAR-3 cell line

The cell lines were grown in RPMI 1640 medium containing 10% fetal bovine serum and 2 mM L-glutamine. For present screening experiment, cells were inoculated into 96 well microtiter plates in 90 µL at 5000 cells per well. After cell inoculation, the microtiter plates were incubated at 37 °C, 5% CO_2, 95% air and 100 % relative humidity for 24 h prior to addition of experimental drugs. Experimental drugs were dissolved in appropriate solvent to prepare stock solutions. At the time of experiment four 10-fold serial dilutions were made using complete medium. Aliquots of 10 µL of these different drug dilutions were added to the appropriate micro-titer wells already containing 90 µL of medium, resulting in the required final drug concentrations. After addition of compound, plates were incubated at standard conditions for 48 h and assay was terminated by the addition of cold TCA. Cells were fixed *in situ* by the gentle addition of 50 µL of cold 30 % (w/v) TCA (final concentration, 10 % TCA) and incubated for 60 minutes at 4°C. The supernatant was discarded; the plates were washed five times with tap water and air dried. Sulforhodamine B (SRB) solution (50 µL) at 0.4 % (w/v) in 1 % acetic acid was added to each of the wells, and plates were incubated for 20 minutes at room temperature. After staining, unbound dye was recovered and the residual dye was removed by washing five times with 1 % acetic acid. The plates were air dried. Bound stain was subsequently eluted with 10 mM rizma base, and the absorbance was read on

an Elisa plate reader at a wavelength of 540 nm with 690 nm reference wavelength. Percent growth was calculated on a plate-by-plate basis for test wells relative to control wells.

$$\text{Percentage growth} = \frac{\text{Average absorbance of the cell test}}{\text{Average absorbance of the control well}} \text{ X } 100$$

Using the six absorbance measurements [time 339 zero (Tz), control growth (C), and test growth in the presence of drug at the four concentration levels (Ti)], the percentage growth was calculated at each of the drug concentration levels. The dose response parameters were calculated for each test article. Growth inhibition of 50 % (GI50) was calculated from [(Ti-Tz)/(C-Tz)] x 100 = 50

This is the drug concentration resulting in a 50% reduction in the net protein increase (as measured by SRB staining) in control cells during the drug incubation. The drug concentration resulting in total growth inhibition (TGI) was calculated from Ti = Tz. The LC50 indicating a net loss of cells following treatment is calculated from

[(Ti-Tz)/Tz] x 100 = -50.

Values were calculated for each of these three parameters if the level of activity was reached; however, if the effect was not reached or was exceeded, the values for that parameter were expressed as greater or less than the maximum or minimum concentration tested.

The results for each test agents are reported as the percentage growth of the tested cells. The compounds that reduce the growth of any one of the cell lines to 32% or less (negative numbers indicates cell kill) are passed on for evolution over a 5-log dose range. In the present screening program all the compounds possessed growth to less than 32% are regarded as active compounds. According to standard NCI protocol, maximum concentration to carry cytotoxic activity is10^{-4} M[34]. Adriamycin was served as positive control compound in the cytotoxic assay. The cell line used in the present investigation is ovary (OVCAR-3).

3. Results And Discussion

The Schiff base is less soluble in ethanol, methanol and highly soluble in acetone, DMF and DMSO while all the nickel(II) complexes are soluble only in DMSO. The purity of all the ligands and their nickel(II) complexes has been checked by TLC. The analytical and physical data of the Schiff bases and their nickel(II) complexes are highlighted in the Table S1.

3.1. ^{1}H-NMR Spectral Analysis

The ^{1}H-NMR spectra of all Schiff bases were recorded in DMSO-d_6, using tetramethylsilane (TMS) as an internal standard. The ^{1}H-NMR spectra of Schiff bases (HL_1-HL_3) show characteristic azomethine proton singlet at δ 10.62-11.07 ppm. The signal at δ 13.27-13.64 ppm is ascribed to -SH proton. The aromatic protons of Schiff bases appeared as a multiplet at δ 7.27-8.29 ppm. The singlet on account of -CH_3 is observed at δ 2.22-2.39 ppm and singlet due to isomeric =C-CH_3 is observed at δ ~2.6 ppm (Fig $S_1$and S_2). Since nickel(II) complexes are paramagnetic; their ^{1}H-NMR spectra could not be obtained [35]. The representative ^{1}H-NMR spectra of HL_1 is shown in Fig 1.

3.2. FT-IR Spectral Studies

The characteristic FT-IR bands of the Schiff bases (HL_1-HL_3) and their nickel(II) complexes (C_1-C_3) are shown in Table S_2. By comparing the infrared spectra of the complexes with those of free ligands one may conclude, ligand molecules exhibit thione ↔ thiol tautomerism. In the spectra of free ligands, the presence of a band at 3067-3096 cm^{-1} and 2753-2770 cm^{-1} assigned to (N-H) and (S-H) vibrations respectively[36] (Fig S_3 (a-c)) which indicates the establishment of thione ↔ thiol tautomeric system. The deprotonation of thiol group and complexation through sulfur atom is indicated by way of the absence of a band within the range 2753-2770 cm^{-1} in the spectra of complexes In the spectra of Schiff bases, a band due to tautomeric form of >C=S is regarded at 1114-1176 cm^{-1}, in metal complexes this peak was absent. The (M-S) vibration seems in the range 332-379 cm^{-1} in the spectra of complexes[37]. The strong band at 1552-1590 cm^{-1} corresponding to azomethine group (C=N) in the spectra of free ligand was shifted to lower wave number in complexes indicating new bond between azomethine and metal ion[38]. This coordination is further confirmed by the presence of a band in the range 483-491 cm^{-1} in complexes assigned to (M-N) vibrations[39]. A broad band at 3311-3200 cm^{-1} indicates the presence of coordinated water molecules. The presence of a water molecule was additionally confirmed with the aid of thermal analysis. FT-IR of C_1 metal complex is shown in (Fig S_3 (d)).

3.3. Electronic and magnetic moment studies

The electronic spectra of Schiff bases (HL_1 - HL_3) and their nickel(II) complexes (C_1 - C_3) have been recorded at room temperature by using DMSO as a solvent (Fig S_4 (a-f)). The electronic spectrum of Schiff bases suggests a band at 335 - 352 nm which may be assigned to n→π* transition of azomethine group. This transition in metal complexes was shifted to lower frequency indicates that imine nitrogen is involved in the coordination of metal ion.

All the nickel(II) complexes exhibits three absorption bands at 990-1012 nm(γ_1), 580-620 nm(γ_2) and ~400 nm(γ_3)[40-42]. These peaks assigned to $^3A_{2g}$ (F) →$^3T_{2g}$ (F) (γ_1), $^3A_{2g}$ (F) → $^3T_{1g}$ (F) (γ_2), and $^3A_{2g}$ (F) → $^3T_{1g}$ (P) (γ_3) transitions respectively which indicates the distorted octahedral geometry for nickel(II) ion. The nickel complexes show off a magnetic moment 3.23-3.45 BM, recommended distorted

octahedral geometry[43]. The electronic spectral data and magnetic moment values of nickel(II) complexes are summarized in Table S_3.

3.4 Mass Spectroscopy

The mass spectrum of ligand (HL_1) and complex (C_1) exhibits parent peak due to molecular ion (M+1). The proposed molecular formulation of these compounds used to be proven through comparing their molecular formula weight with m/z value. The molecular ion peak used to be acquired at m/z 264 for ligand and m/z 620 for complex. This worth is in excellent agreement with the proposed molecular components of compounds. A mass spectrum of HL_1 and C_1 is exhibited in Fig S_5 (a-b).

3.5. Thermal Analysis

In thermal analysis, it is observed that, the nickel(II) complexes decomposes in three ranges (Table 1). The first range is within 120 - 190^oC consequences in the mass loss of coordinated water molecules of hydration. Then the anhydrous complexes decompose in a major stage consisting of two overlapping steps. In the first stage, the organic part started decomposing, leaving metal-triazole at 180-455^oC. In the temperature range of 400-560°C, all the triazole parts get decomposed. The decomposition of the complexes ended with nickel oxide formation above 550^oC. These observations are matched with existing literature[44]. The thermogram of C_1 is represented in Fig S_6.

3.6 *X-ray diffraction analysis*

The X-ray powder diffraction method is broadly used as an experimental technique to purpose of crystal structure. It is more suitable for identification and determination of crystal structure of high symmetry. The X-ray diffraction of compounds was carried out in the range 5-100^o at wavelength of 1.54060 Å. The diffractogram and associated data describe the 2θ value for each peak, relative intensity and inter planar spacing. The diffractogram of HL_1 had nine reflections between 20-60^o with maximum at 2θ=26.6576^o corresponding to d=3.34404Å. The diffractogram of HL_2 shows eleven reflections with maximum at 2θ=11.3588^o corresponding to d value 7.92995Å. The diffractogram of HL_3 had eleven reflections with maxima at 2θ=11.3588^o corresponding to d value 7.79024Å. The diffractogram of C_3 had eleven reflections with maxima at 2θ=7.4380^o corresponding to d value 11.88565Å. The X-ray diffraction pattern of these compounds with respect to major peaks having relative intensity 100% has been indexed by using computer programme. The above indexing method also yields Miller indices (*hkl*), unit cell parameters and unit cell volume. The X-ray diffraction spectra of all compounds are shown in Fig S_7 (a-d) and their d values, FWHM and relative intensities are given in Table S_4 (a-d). Also X-ray parameters are listed in Table 2. In concurrence with cell parameters, the conditions such as $a \neq b \neq c$ and $\alpha=\beta=\gamma=90^o$ required for samples to be orthorhombic were tested and found to be satisfactory. Hence, it can be concluded that all the compounds have orthorhombic crystal system[45]. The experimental density values for all the ligands and their metal complexes were determined by using standard specific gravity

method[46, 47] and found to be 0.7512, 0.2016, 0.61and 0.47 g/cc for HL_1, HL_2, HL_3 and HL_3-Ni, respectively. By using experimental density values, molecular weight, Avogadro's number, volume of the unit cell, the number of molecules per unit cell were calculated using the equation ρ = ηM/NV and was found to be one, one, two, one for HL_1, HL_2, HL_3 and HL_3-Ni, respectively. With these values theoretical densities were computed and found to be 0.8239, 0.2265, 0.65 and 0.52 g/cc for the respective compounds. The comparison of experimental and theoretical density values shows good agreement within the limits of experimental error[48].

To calculate pore fraction 'P' the experimental and theoretical densities of sample are needed. The pore fraction 'P' is determined by relation P=1-(Experimental density/Theoretical density). By substituting density values, 'P' was calculated. The P values are observed 0.0853, 0.1099, 0.0599 and 0.0961 for the respective compounds. In fact this approximation is not sufficient for exact picture of pore fraction parameter, but this value is very important in obtaining information about inhomogeneity of sample. Other method to study inhomogeneity of sample is related with the average particle size. The average particle size (Crystallite size) was calculated using line broadening with Debye-Scherrerequation. D=0.9λ/βCosθ. The crystallite size is observed 337, 169, 337 and 235 Å for the respective compounds. Micro strain is calculated as Microstrain=βCosθ/4 and found to be 1.2649 $x10^{-3}$, 219 $x10^{-3}$, 1.024 $x10^{-3}$ and 1.376 $x10^{-3}$ for the respective compounds. The space group of all compounds was confirmed by referring to earlier reported reference[46, 49].

3.7 In vitro antimicrobial and antifungal activities

The results are summarized in Table 3. All the Schiff bases (HL_1- HL_3) and nickel(II) complexes (C_1-C_3) are inactive against *Aspergillus niger.* The ligand is weakly active against *Pseudomonas aeruginosa and Candida albicans* while moderate to highly active against *Staphylococcus aureus*. All the nickel(II) complexes are moderate to highly active against bacteria and moderately active against *Candida albicans*. The results were compared with standard drugs like Gentamycine and Streptomycin. The compounds are less potent as compare to standard drugs.

Similar procedure was repeated for antifungal activities; the MGYP agar plates were prepared using submerged inoculation using fungal strain *Candida albicans* (NCIM 3466). The agar plates were incubated at 27 °C temperature for 48 to 72 hrs. After incubation plates were examined for zone of inhibition around wells as shown in Fig 2.

3.8. Molecular docking studies

In order to understand the possible mode of action of the synthesized metal complex, the molecular docking analysis was carried out using crystal structure of the Human CDK7. Docking analysis revealed that HL_1 (GI50>100 μM) is interacting with the selected protein target with formation of the only one hydrogen bond interaction with GLN22 and hydrophobic interaction with the amino acids like LYS41, VAL36 with total docking score of -40.52 k $Calmol^{-1}$. C_1 complex (GI50=66.7 μM) was found to have

docking score of -84.53 k Cal mol^{-1} and interacted via formation of one hydrogen bond interaction with ASN142, charge interaction with GLU99, ASP97 and hydrophobic interactions with GLY21 and GLU99. HL_2 (GI50>100 μM) was found to be showing docking score of -47.89 k Cal mol^{-1} and interacted via formation of two hydrogen bond interactions with PHE23, SER97, aromatic interaction with TRP43, PHE51, PHE122, van der Waals interactions with TYR18, PHE40, TRP43, SER44 etc. and hydrophobic interaction with LEU144, GLU121, PHE122, ALA125. HL_2-Ni (GI50=67.7 μM) complex interacted via formation of one hydrogen bond interaction with ASN142, charge interaction with GLU99 and hydrophobic interaction with LYS103,ASN144 with total docking score of -96.35 k Cal mol^{-1}. HL_3 (GI50>100μM) showed docking score of -47.89 k Cal mol^{-1} and interacted via formation of hydrogen bond interaction with PHE23 and hydrophobic interaction with LEU144, LYS41. The C_3 complex (GI50>100 μM) was found to have docking score of -88.76 k Cal mol^{-1} and showed one hydrogen bond interaction with LYS139, charge interaction with ASP97 and hydrophobic interaction with LYS139, VAL100. Docking analysis indicated the developed ligands are having ability to bind with the Human CDK7 which can be possible mode of the action for anticancer potential.

The binding energy and critical interactions of all Schiff bases (HL_1- HL_3) and their nickel(II) complexes (C_1-C_3) are exhibited in the Table 4. The interactions of HL_1 and C_1 with amino acid are exhibited in Fig 3(a-b) respectively.

3.7. Effect of Ligands (HL_1 -HL_3) and its complexes (C_1-C_3) on antiproliferative activity

The growth curve of human ovarian cancer cell line OVCAR-3 for Schiff bases (HL_1- HL_3) and their nickel(II) complexes (C_1-C_3) is represented in Fig 4. All the synthesized compounds were screened for their anticancer activity against OVCAR-3 (ovary) cell line. The anticancer activity was measured *in vitro* for the newly synthesized Schiff bases (HL_1-HL_3) and nickel(II) complexes (C_1-C_3) using the Sulforhodamine B stain (SRB) assay method[50-52]. In the current protocol, each cell line is inoculated on a pre-incubated microtiter plate. The test agents are added at a single concentration and the culture is incubated for 48 h. The endpoint of determinations is made with Sulforhodamine B, a protein-binding dye. The results for each test agent are reported as the percentage growth of the tested cells. The average values for % control growth for the cell line OVCAR-3 are listed in Table 5 and cytotoxicity for the same cell line is as shown in Table 6.

The results concern with average values for % control growth suggests that all the Schiff bases are inactive against ovarian cancer cell line OVCAR-3 at all concentrations but C_1 and C_2 are active at 10^{-4} mol L^{-1} concentration. C_2 is more active than C_1 at 10^{-4} mol L^{-1} concentration. The C_3 does not show any activity. Based on GI50 value all the Schiff bases are inactive while C_1 (GI50 = 66.7 x 10^{-6}mol L^{-1}) and C_2 (GI50 = 67.7 x 10^{-6}mol L^{-1}) are moderately active against ovarian cancer cell line OVCAR-3. C_3 is inactive. The correlation plot of binding energy and GI50 for active compounds (C_1 and C_2) is represented in Fig S_8.

3.8 Structure activity Relationship (SAR studies)

In general, synthesized nickel(II) complexes are found to be active against OVCAR-3 cell lines at a molar dose of 10^{-4} mol L^{-1} which indicates their anticancer potential. The SAR analyses of the synthesized complexes are indicated in the following:

- 1, 2, 4-Triazoles with methyl substituent were moderately active against cancer cell lines. The nickel complexes of HL_1 and HL_2 are showed GI50 value 66.7μM and 67.7μM respectively, which indicates the substitution of the good electron-withdrawing group like $-NO_2$ sufficiently affecting the polarity of the molecules.
- The position of the $-NO_2$ group is also an important parameter in the biological activity of these derivatives, 3 and 4 substituted derivatives are more potent than the corresponding 2 substituted ones. This might be due to the loss of favourable conformation in ortho-substituted derivatives.

4. Conclusions

The synthesized Schiff bases act as a bidentate ligand and coordinated to the nickel(II) ion through nitrogen and sulphur of the thiol group. The binding of ligand to a metal ion is confirmed by elemental analysis, spectral studies (UV-visible, IR, ^{1}H NMR), TGA, magnetic moment measurement. The Ni(II) complexes are found to exhibit octahedral geometry. All the Schiff bases (HL_1-HL_3) and Ni complexes are inactive against *Aspergillus niger* but metal complexes are more effective against *Staphylococcus aureus, Pseudomonas aeruginosa* and *Candida albicans*. The anticancer results shows that, nickel(II) complexes exhibit as a quality anticancer agent.

Declarations

Author Contributions

Conceptualization, Methodology and Investigation: Sachin A. Deodware; Software and Validation: Kundalkesha S. Gaikwad; Formal analysis and Data curation: Umesh B. Barache; Resources: Umakant B. Chanshetti; Supervision: Shashikant H. Gaikwad; Writing-original draft preparation: Pratibha C. Dhale; Writing-review and editing: Panchsheela A. Ubale;

Acknowledgements

The authors gratefully acknowledge the ACTREC, Tata memorial center, Kharghar, New Mumbai, India for providing anticancer activity. We also acknowledge Dr. P.P. Wadgaonkar, NCL, Pune, India for their kind co-operation.

The author has no conflict of interest.

References

1. Baklale R, Naik GN, Mangannavar CV, et al. *Eur. J Med Chem* 2014; 73: 38. DOI:10.1016/j.ejmech.2013.11.037
2. Junior WB, Alexandre-Moreira MS, Alves MA, et al. *Molecules* 2011; 16(8): 6902. DOI:10.3390/molecules16086902
3. Inam A, Siddiqui SM, Macado TS et al. *Eur J Med Chem* 2014; 75: 67. DOI: 10.1016/j.ejmech.2014.01.023
4. Mohamed GG, Zayed EM and Hindy AMM. *Spctrochim Acta A, Molecular and Biomolecular Spectroscopy* 2015; 145: 76. DOI: 10.1016/j.saa.2015.01.129
5. Almeida A, Oliveira BL, Correia JDG, et al. *Coord Chem Rev* 2013; 257: 2689. DOI: 16/j.ccr.2013.01.031
6. Turan-Zitouni G, Kaplancikli ZA, Yildiz MT, et al. *Eur J Med Chem* 2005; 40(6): DOI: 10.1016/j.ejmech.2005.01.007
7. Wu WN, Jiayang YM, Fei Q, et al. Phosphorus, Sulfur, and Silicon and the Related Elements 2019; 194(12): 1171. DOI: 10.1080/10426507.2019.1633321
8. Koparir P. *Phosphorus, Sulfur,* and Silicon and the Related Elements 2019; 194(11): 1. DOI: 10.1080/10426507.2019.1597363
9. Cui XS, Chen J, Chai KY, et al. *Med Che. Res* 2009; 18: 49. DOI:10.1007/s00044-008-9106-3.
10. Sujith, KV, Rao JN, Shetty P and Kalluraya B. *Eur Med Chem* 2009; 44: 3697. DOI: 10.1016/j.ejmech.2009.03.044
11. Kamble UV, Patil SA and Badami PS. *J Inc. Phenom Macrocycl Chem* 2010; 68(3)*:* DOI: 10.1007/s10847-010-9794-4
12. Almasirad A, Shafiee A, Abdollahi A, et al. *Med Chem Res* 2011; 20: 435. DOI:10.1007/s00044-010-9335-0
13. Tyagi P, Chandra S, Saraswat BS, et al. *Spectrochim Acta A* 2015; 145:155. DOI: 10.1016/j.saa.2015.03.034.
14. Abd-Rabou AA, Abdel-Wahab BF and Bekheit MS. *Chem Pap* 2018; 72(9): 2225. DOI: 10.1007/s11696-018-0451-5
15. Kumar P, Narsimhan B and Sharma D. *ARKIVOC;* 2008: xiii*,* 159. DOI: arkat-usa.org/get-file/25663
16. Kumar D, Judge V, Narang R, et al. *Eur J Med Chem* 2010; 45(7): 2806. DOI: 10.1016/j.ejmech.2010.03.002
17. Shaikh AB, Barache UB, Anuse MA, et al. *S Afr J Chem* 2016; 69: 157. DOI:10.17159/0379-4350/2016/v69a19
18. Shaikh AB, Barache UB, Lokhande TN, et al. *Rasayan J Chem* 2017; 10: 967. DOI:admin/php/upload/236_pdf.pdf
19. Barache UB, Shaikh AB, Deodware SA, et al. *Int. J Environ Anal Chem* 2019; 99: DOI:10.1080/03067319.2019.1607316

20. Barache UB, Shaikh AB, Lokhande TN, et al. *Spectrochim ActaA* 2018; 189: 443 DOI:10.1016/j.saa.2017.08.054
21. Barache UB, Shaikh AB, Lokhande TN, et al. *J Environ Chem Eng* 2017; 5: 4828. DOI: https://doi.org/10.1016/j.jece.2017.09.021
22. Barache UB, Khogare BT, Shaikh AB, et al. *Chem Data Coll* 2019; 19: 10073 DOI:10.1016/j.cdc.2018.100173
23. Barache UB, Shaikh AB, Deodware SA, et al. *Ground water Sust Dev* 2019; 9: 100221. DOI:10.1016/j.gsd.2019.100221
24. Capranico G, Zagotto G and Palumbo M. *Curr Med Chem* 2004; 4: 335. DOI: 10.2174/1568011043352885
25. Bryant SG and Ereshefsky L. *Clin. Pharm*. 1982, *1(5)*, 406-417. DOI: ncbi.nlm.nih.gov/6764164
26. Stahl SM.*CNS Spectr* 2008; 13(12): 1027.DOI: 10.1017/s1092852900017089.
27. Deodware SA, Sathe DJ Gaikwad SH, et al. *Arabian J Chem*, 2017; 10: 262. DOI: 10.1016/j.arabjc.2016.09.024
28. Bala S. Gupta RP Sachdeva ML, Singh A, et al. *Indian J Chem* 1978; 16: 481.
29. Durairaja S, Srinivasan S and Perumalsamy PL. *Electron J Biol* 2009; 5(1): 5.
30. Bowrsand EF and Jeffries LR. *J Clin Pathol* 1955; 8: 58.
31. Meng XY, Zhang HX, Mezei M, et al. *Curr Comput Aided Drug Des* 2011; 7: 146. DOI: 10.2174/157340911795677602
32. López-Vallejo F, Caulfield T, Martínez-Mayorga K, et al. *Comb Chem High Throughput Screen* 2011; 14(6): 475. DOI: 10.2174/138620711795767866.
33. Huang SY and Zou X. *Int J Mol Sci* 2010; 11(8): 3016. DOI: 10.3390/ijms11083016
34. Holla BS, Rao BS, Sarojini BK, *Eur J Med Chem* 2006; 41: 657.
35. Canpolat E and Kaya M. *Turk J Chem* 2005; 29(4): 409.
36. Gudasi KB, Patil SA, Vadavi, RS, et al. *Transition Met Chem* 2005; 30(8): 1014. DOI: 10.1007/s11243-005-6297-z
37. Chandan S and Gupta K. *Transition Met Chem*; 2002; 27: 196.
38. Singh K, Singh DP, Barwa MS, et al. *J Enz Inhib Med Chem*; 2006; 21(5): 557. DOI: 10.1080/14756360600642131
39. Nakamoto K. *Infrared and Raman Spectra of Inorganic and Coordination Compounds*; 1997: John Wiley and Sons Inc: New York: USA.
40. Khlood S and Melha-Abou. *J Coord Chem* 2008; *61*: 2053. DOI: 10.1080/00958970701862167
41. Mahapatra BB, Raval MK, Behera AK et al. *J Indian Chem Soc* 1995; 72: 161.
42. Cotton FA, Wilkinson G, Murillo CA and Bochmann, M. *Advanced Inorganic Chemistry* 2003; Wiley: New York: USA.
43. Bagihalli GB and Patil SA. *J Enz Inhib Med Chem* 2010; 25: 430. DOI:10.3109/14756360903257876

44. Singh K, Barwa MS and Tyagi P. *Eur J Med Chem* 2006; 41: 147. DOI:10.1016/j.ejmech.2005.06.006
45. Shelke VA, Jadhav SM, Patharkar VR Shankarwar SG, et al. *Arabian J Chem* 2012; 5(4): 50. DOI: 10.1016/j.arabjc.2010.09.018
46. Pattar RT, Choukimath KRand Tulsigiri VG. *Indian J Phy* 1993; 73: 343.
47. Shoemaker DP and Garland CW. *Experiments in Physical Chemistry*, McGraw Hill International edition, New York: USA, 1989.
48. Deshmukh MB, Dhongade Desai S and Chavan SS. *Ind J Chem* 2005; 44B: 1659. DOI:nopr.niscair.res.in/bitstream/123456789/9153/1/IJCB%2044B%288%29%201659-1662.
49. Cullity BD. Addison Wesley Pub. Co. INC, Massachusetts: USA, 1956.
50. Grever RM, Schepartz SA and Chabner BA. *Semin Oncol* 1992; 19(6): 622. PMID: 1462164
51. Boyd M R. *Anticancer Drug Development Guide: Preclinical Screening, Clinical Trials and Approval* 2004; Human Press Inc, New Jersey: USA.
52. Vichai V and Kirtikar K. *Nat Prtoc* 2006; 1: 1112. DOI:10.1038/nprot.2006.179

Figures

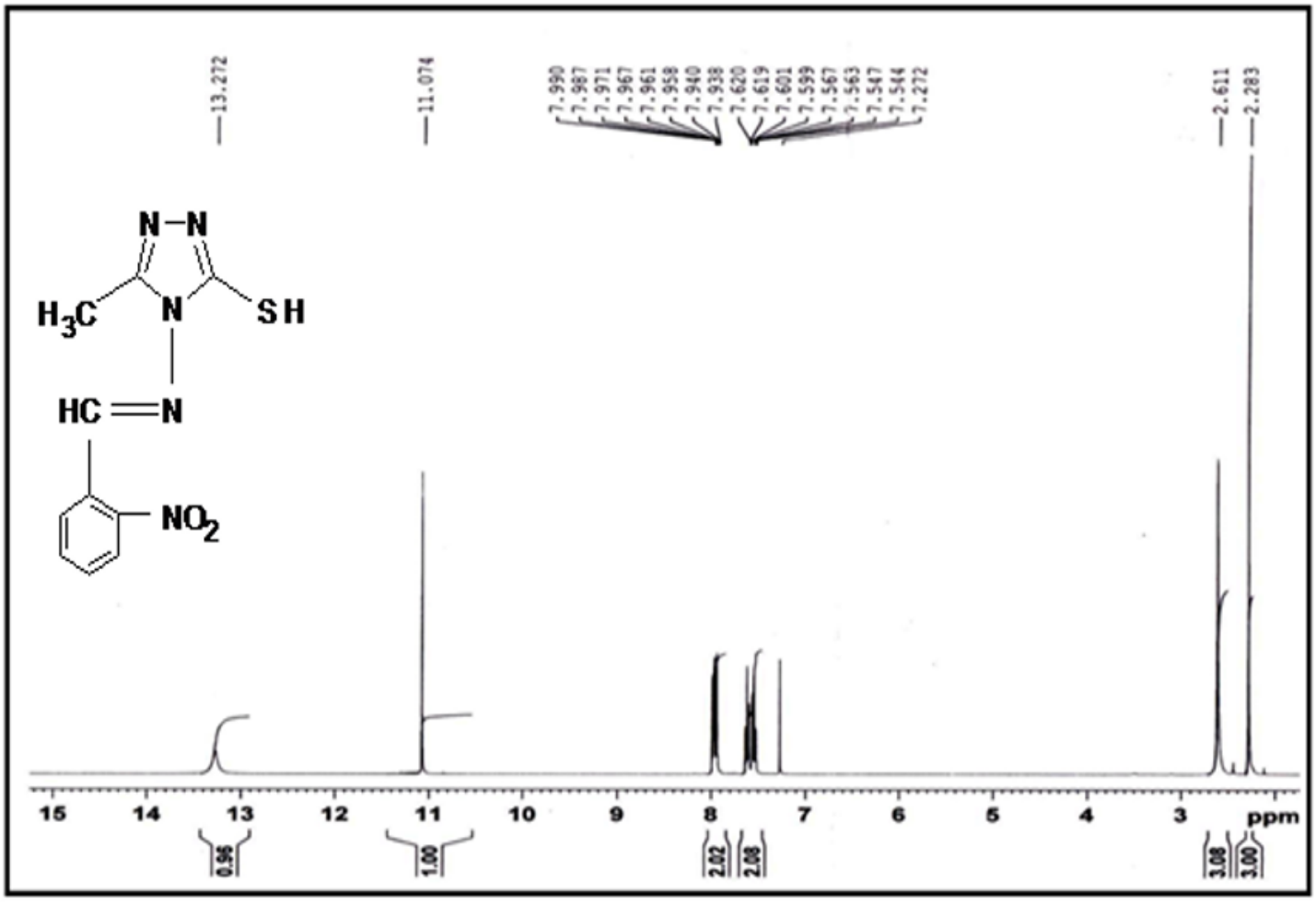

Figure 1

1H-NMR of HL1: 4-(2□-Nitrobenzelideneimino)-3-methyl-5-mercapto-1,2,4- Triazole

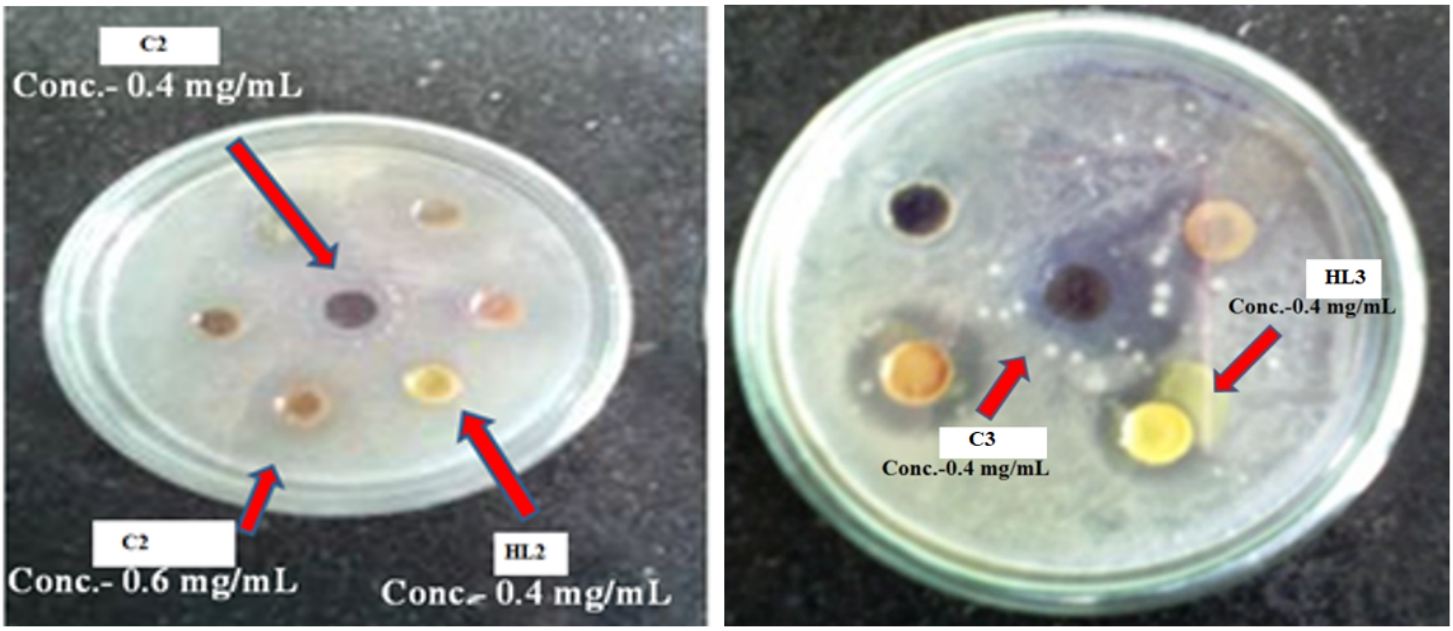

Figure 2

: (a) Zone of inhibition of HL2 and C2 for Pseudomonas aeruginosa (b) Zone of inhibition of HL3 and C3 for Staphylococcus aureus

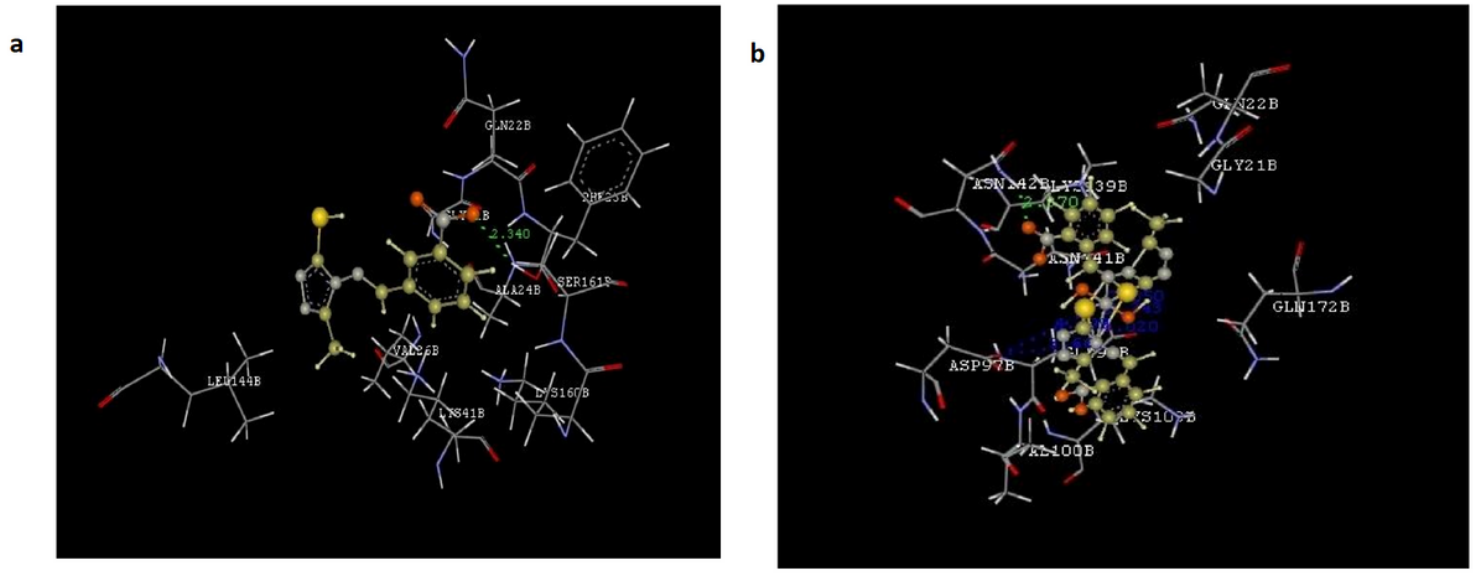

Figure 3

(a) Interactions of HL1 with amino acid. (b) Interactions of C1 with amino acid

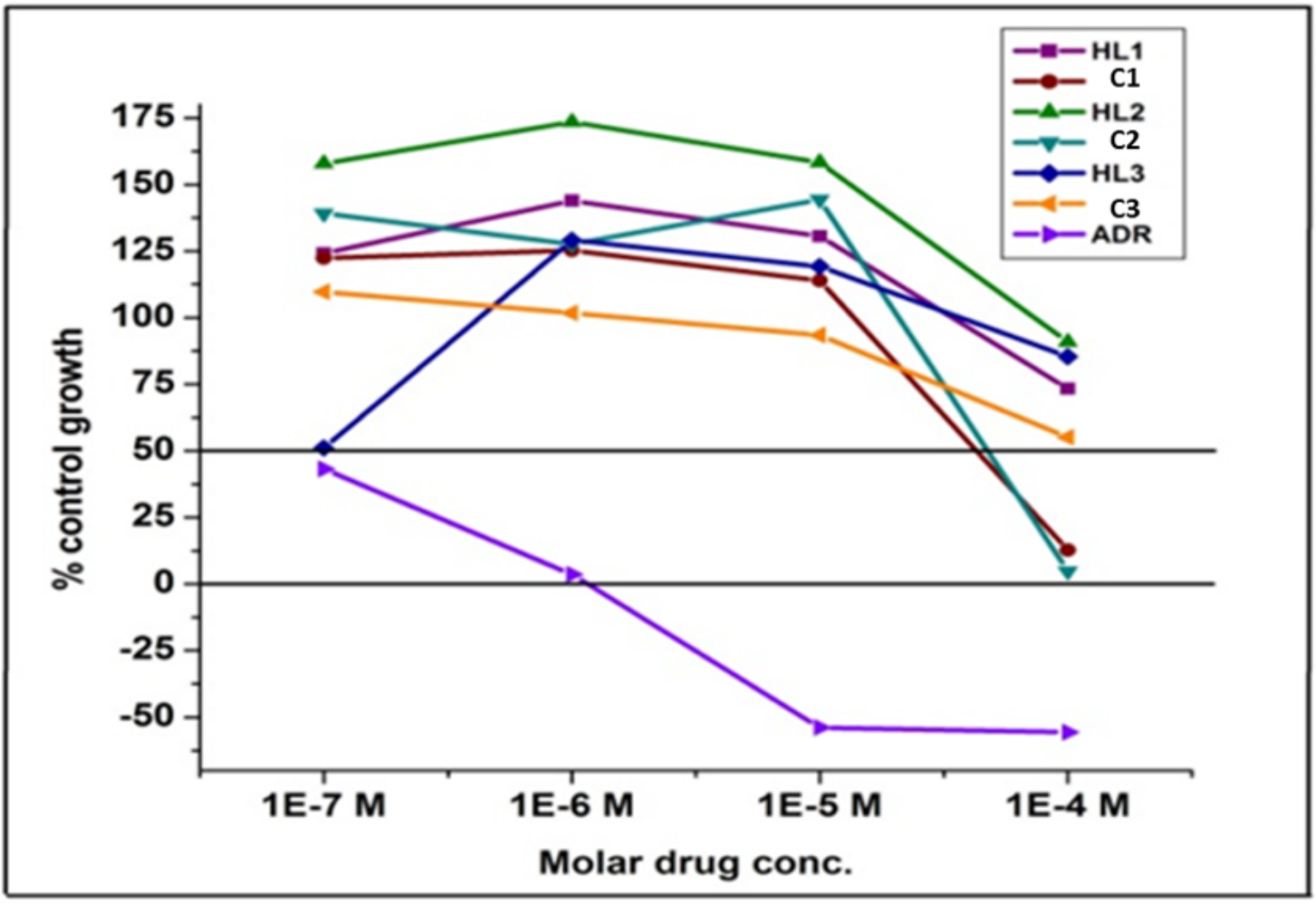

Figure 4

Growth curve for human ovarian cancer cell line OVCAR-3 for Schiff bases and their nickel(II) complexes

Supplementary Files

This is a list of supplementary files associated with this preprint. Click to download.

- Scheme1.png
- GraphicalAbstract.docx
- supportinginformation200321.docx